

Josephson current in a superconductor-ferromagnet junction with two noncollinear magnetic domains

B. Crouzy,¹ S. Tollis,¹ and D. A. Ivanov¹

¹*Institute for Theoretical Physics, École Polytechnique Fédérale de Lausanne (EPFL), CH-1015 Lausanne, Switzerland*
(Dated: July 30, 2018)

We study the Josephson effect in a superconductor–ferromagnet–superconductor (SFS) junction with ferromagnetic domains of noncollinear magnetization. As a model for our study we consider a diffusive junction with two ferromagnetic domains along the junction. The superconductor is assumed to be close to the critical temperature T_c , and the linearized Usadel equations predict a sinusoidal current-phase relation. We find analytically the critical current as a function of domain lengths and of the angle between the orientations of their magnetizations. As a function of those parameters, the junction may undergo transitions between 0 and π phases. We find that the presence of domains reduces the range of junction lengths at which the π phase is observed. For the junction with two domains of the same length, the π phase totally disappears as soon as the misorientation angle exceeds $\frac{\pi}{2}$. We further comment on the possible implication of our results for experimentally observable 0– π transitions in SFS junctions.

I. INTRODUCTION

The interest in proximity structures made of superconducting and ferromagnetic layers (respectively, S and F) in contact with each other has been recently renewed due their potential applications to spintronics¹ and to quantum computing.^{2,3} The interplay between superconductivity (which tends to organize the electron gas in Cooper pairs with opposite spins) and ferromagnetism (which tends to align spins and thus to destroy the Cooper pairs) leads to a variety of surprising physical effects (for a review, see Ref. 4). As a consequence of the exchange splitting of the Fermi level,⁵ the Cooper pair wave function shows damped oscillations in the ferromagnet, leading to the appearance of the so-called “ π state” in SFS junctions.⁶ In the π state, the superconducting order parameter is of opposite sign in the two S electrodes of the Josephson junction, and thus a macroscopic superconducting phase difference of π appears in the thermodynamic equilibrium. This phase difference should lead to spontaneous nondissipative currents in a Josephson junction with annular geometry.⁷ A possible signature for the π -state appearance is a cancellation of the Josephson critical current followed by a reversal of its sign as a function of the junction length.⁴ The recent experimental observations of critical-current oscillations in experiments^{8,9,10,11} have demonstrated such 0– π transitions as a function of the ferromagnet thickness and temperature.

The appropriate formalism to deal with mesoscopic S/F junctions has been derived by Eilenberger.¹² The equations of motion for the quasiclassical Green function (averaged over the fast Fermi oscillations) can be further simplified in the diffusive regime, *i.e.*, when the motion of the electrons is governed by frequent scattering on impurity atoms: the Green functions can then be averaged over the momentum directions. This averaging is justified as long as the elastic mean free path l_e is much smaller than the relevant length scales of the system, namely the size of the layers, the superconducting coherence length $\xi_S = \sqrt{D/2\pi T_c}$, and the length characterizing the Cooper pair wave function decay in the ferromagnet $\xi_F = \sqrt{D/\hbar}$. Here and in the following, D denotes the diffusion constant, T_c the superconducting critical temperature, \hbar the magnitude of the exchange field, and the system of units with $\hbar = k_B = \mu_B = 1$ is chosen. The diffusive limit is reached in most of the experimental realizations of S/F heterostructures. In this limit, the Green functions can be combined in a 4×4 matrix in the Nambu \otimes spin space, and this matrix obeys the Usadel equations.¹³ SFS Josephson junctions with homogeneous magnetization have been studied in detail within this framework.⁴ Close to T_c , the proximity effect is weak, the Usadel equations can be linearized, and the current-phase relation is sinusoidal¹⁴

$$I_J = I_c \sin \phi, \quad (1)$$

where ϕ is the superconducting phase difference across the junction. The critical current I_c shows a damped oscillatory dependence on the F-layer thickness (for a review, see Refs. 15 and 16).

However, understanding the effect of a nonhomogeneous magnetization is of crucial interest for obtaining a good quantitative description for the critical-current oscillations in SFS junctions. Indeed it is known that real ferromagnetic compounds usually have a complex domain structure. Strong ferromagnets (such as Ni or Fe) consist of domains with homogeneous magnetization pointing in different directions whereas the magnetic structure of the weak ferromagnets (Cu-Ni and Pd-Ni alloys) used in the experiments reported in Refs. 8,9,10,11 is still not known precisely. The problem of SFS junctions with inhomogeneous magnetization has been addressed previously for spiral magnetizations¹⁷ and in the case of domains with antiparallel (AP) magnetizations.^{18,19} In the latter case, the critical-current oscillations

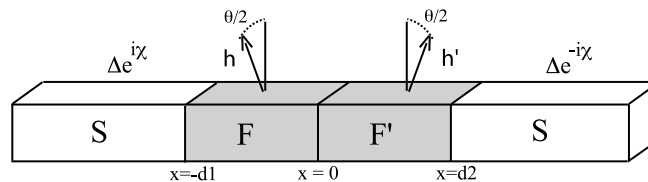


FIG. 1: S-FF'-S junction with non-collinear magnetization.

(and thus the π state) are suppressed in the symmetric case where the F layer consists of two domains of the same size. This can be explained by a compensation between the phases acquired by the Andreev reflected electrons and holes, of opposite spins, in the two domains.¹⁸

In the present paper, we extend that analysis to the case of a SFF'S junction close to T_c , with the two magnetic domains F and F' of arbitrary length and relative orientation of the magnetizations. To emphasize the effect of the misorientation angle between the magnetizations of the two domains, we choose to minimize the number of parameters in the model. The interfaces are then chosen to be perfectly transparent, and spin-flip scattering is neglected in both S and F layers. Furthermore, we assume that the diffusive limit is fully reached, that is we do not take into account corrections due to a finite mean free path (note that for strong ferromagnets the magnetic coherence length ξ_F may become comparable to l_e).

The main result of our calculation is that, in the symmetric case where the two domains have equal thicknesses, we obtain a progressive reduction of the π -state region of the phase diagram as the misorientation angle increases. Surprisingly, the π state completely disappears as soon as the misorientation angle θ exceeds $\frac{\pi}{2}$.

The paper is organized as follows. In Section II we solve the linearized Usadel equations and give the general expression for the Josephson current. In Section III we discuss the simplest cases of parallel and antiparallel relative orientation of magnetizations with different domain sizes d_1 and d_2 . We obtain analytically the full phase diagram in d_1 - d_2 coordinates. In agreement with Ref. 18, the π state is absent in the symmetric case $d_1 = d_2$ for domains with antiparallel magnetizations. In the asymmetric case, the critical current oscillates as d_2 is varied while keeping d_1 constant. For sufficiently thick layers ($d_{1,2} \gg \xi_F$), the critical-current oscillations behave like in a single domain of thickness $|d_1 - d_2| + (\pi/4)\xi_F$. In Section IV, we discuss the case of an arbitrary misorientation angle in the symmetric configuration $d_1 = d_2 = d$. In the limit when the exchange field is much larger than T_c , we derive analytically the 0 - π phase diagram of the junction depending on the junction length d and on the misorientation angle θ . We show that the π state disappears completely for $\theta > \frac{\pi}{2}$. In the last section V, we discuss possible implications of our findings for experimentally observed 0 - π transitions in SFS junctions.

II. MODEL

We study a diffusive SFF'S Josephson junction with semi-infinite (that is, of thickness much larger than ξ_S) superconducting electrodes, as shown in Fig. 1. The phase difference between the S-layers is denoted $\phi = 2\chi$, the thicknesses of the two ferromagnetic domains d_1 and d_2 . In the following we consider a quasi-one-dimensional geometry where the physical quantities do not depend on the in-plane coordinates. For simplicity, we assume that the S-F and F-F' interfaces are transparent. We further assume that the temperature is close to T_c so that $\Delta \ll T$, and this allows us to linearize the Usadel equations.

In the case of superconducting-ferromagnet systems, the proximity effect involves both the singlet and the triplet components of the Green's functions.²⁰ The Usadel equation in the ferromagnetic layers takes the form (we follow the conventions used in Ref. 21)

$$D\nabla(\check{g}\nabla\check{g}) - \omega[\hat{\tau}_3\hat{\sigma}_0, \check{g}] - i[\hat{\tau}_3(\mathbf{h} \cdot \hat{\sigma}), \check{g}] = 0. \quad (2)$$

The Green function \check{g} is a matrix in the Nambu \otimes spin space, $\hat{\tau}_\alpha$ and $\hat{\sigma}_\alpha$ denote the Pauli matrices respectively in Nambu (particle-hole) and spin space, $\omega = (2n + 1)\pi T$ are the Matsubara frequencies and \mathbf{h} is the exchange field in the ferromagnet. The Usadel equation is supplemented with the normalization condition for the quasiclassical Green function

$$\check{g}^2 = \check{\mathbf{1}} = \hat{\tau}_0\hat{\sigma}_0. \quad (3)$$

For simplicity, we assume that the superconductors are much less disordered than the ferromagnets, and then we can

impose the rigid boundary conditions at the S/F interfaces:

$$\check{g} = \frac{1}{\sqrt{\omega^2 + \Delta^2}} \begin{pmatrix} \omega & \Delta e^{\pm i\chi} \\ -\Delta e^{\mp i\chi} & -\omega \end{pmatrix}_{\text{Nambu}} \otimes \hat{\sigma}_0, \quad (4)$$

where Δ denotes the superconducting order parameter and the different signs refer respectively to the boundary conditions at $x = -d_1$ and $x = d_2$.

Close to the critical temperature T_c , the superconducting correlations in the F region are weak,⁴ and we can linearize the Usadel equations (2),(3) around the normal solution $\check{g} = \hat{\tau}_3 \hat{\sigma}_0$. The Green's function then takes the form

$$\check{g} = \begin{pmatrix} \sigma_0 \text{sgn}(\omega) & f_\alpha \sigma^\alpha \\ -f_\alpha^\dagger \sigma^\alpha & -\sigma_0 \text{sgn}(\omega) \end{pmatrix}, \quad (5)$$

where the scalar f_0 (respectively f_0^\dagger) and vector \mathbf{f} (respectively \mathbf{f}^\dagger) components of the anomalous Green functions obey the linear equations

$$\begin{aligned} \frac{\partial^2 f_\pm^{(\dagger)}}{\partial x^2} - [\lambda_\pm]^2 f_\pm^{(\dagger)} &= 0 \\ \frac{\partial^2 f_\perp^{(\dagger)}}{\partial x^2} - [\lambda_\perp]^2 f_\perp^{(\dagger)} &= 0 \end{aligned} \quad (6)$$

with

$$\lambda_\pm = \left[2 \frac{|\omega| \mp i h \text{sgn}(\omega)}{D} \right]^{1/2}, \quad \lambda_\perp = \left[2 \frac{|\omega|}{D} \right]^{1/2}. \quad (7)$$

The projections of the anomalous Green function on the direction of the exchange field (“parallel” components) are defined as $f_\pm^{(\dagger)}(x) = f_0^{(\dagger)} \pm \mathbf{f}^{(\dagger)} \cdot \mathbf{e}_h$ where \mathbf{e}_h is the unit vector in the direction of the field. The “perpendicular” component $f_\perp^{(\dagger)}$ refers to the axis orthogonal to the exchange field. Generally, this component is a two-dimensional vector. In our system, however, \mathbf{f} lies in the plane spanned by the magnetizations in the two domains, and therefore $f_\perp^{(\dagger)}$ has only one component.

It follows from Eq. (6) that the decay of the “parallel” and the “perpendicular” components is governed by two very different length scales. The parallel component decays on the length scale ξ_F , while the perpendicular component is insensitive to the exchange field and decays on the typically much larger scale $\xi_S = \xi_F \sqrt{\frac{h}{2\pi T_c}}$ (experimentally, h may be more than 100 times larger than T_c , see, e.g., Ref. 11).

In the absence of the exchange field, f_σ and f_σ^\dagger components are related by complex conjugation. The exchange field h breaks this symmetry, and the relation between f_σ and f_σ^\dagger becomes

$$f_\sigma^\dagger(\chi) = f_\sigma(-\chi). \quad (8)$$

The solutions to the equations (6) in each of the ferromagnetic layers are given by

$$f_{\pm,\perp}^j(x) = A_{\pm,\perp}^j \sinh \lambda_{\pm,\perp} x + B_{\pm,\perp}^j \cosh \lambda_{\pm,\perp} x, \quad (9)$$

where the 12 coefficients $A_{\pm,\perp}^j$ and $B_{\pm,\perp}^j$ ($j = 1, 2$ denotes the layer index) must be determined using the boundary conditions at each interface. Note that it is enough to solve the equations for the functions f_σ^j : the functions $f_\sigma^{j\dagger}$ can be then obtained from the symmetry relation (8)

As we assume transparent S/F interfaces and rigid boundary conditions,

$$\begin{aligned} f_\pm^1(x = -d_1) &= \frac{\Delta}{\omega} e^{i\chi} \\ f_\pm^2(x = d_2) &= \frac{\Delta}{\omega} e^{-i\chi} \\ f_\perp^1(x = -d_1) &= f_\perp^2(x = d_2) = 0. \end{aligned} \quad (10)$$

At the (perfectly transparent) F/F' interface, the standard Kupriyanov-Lukichev boundary conditions²² provide the continuity relations

$$\begin{aligned} f_\alpha^1(x = 0) &= f_\alpha^2(x = 0) \\ \frac{\partial f_\alpha^1}{\partial x} \Big|_{x=0} &= \frac{\partial f_\alpha^2}{\partial x} \Big|_{x=0} \end{aligned} \quad (11)$$

(here α takes values 0 to 3 and refers to a fixed coordinate system). Note that, in the general case, since the ferromagnetic exchange fields do not have the same orientation in the two F-layers, the latter conditions do not lead to the continuity of the reduced functions $f_{\pm,\perp}^j$ and their derivative, except in the parallel case.

The last step will be to compute the Josephson current density using the formula²⁰

$$I_J = ieN(0)DS\pi T \sum_{\omega=-\infty}^{\infty} \frac{1}{2} \text{Tr} (\hat{\tau}_3 \hat{\sigma}_0 \dot{g} \partial_x \check{g}), \quad (12)$$

where S is the cross section of the junction, $N(0)$ is the density of states in the normal metal phase (per one spin direction) and the trace has to be taken over Nambu and spin indices. The current can be explicitly rewritten for the linearized \check{g}

$$I_J = -ieN(0)DS\pi T \sum_{\omega=-\infty}^{\infty} \left[\sum_{\sigma=\pm} \frac{1}{2} (f_{\sigma} \partial_x f_{\sigma}^{\dagger} - f_{\sigma}^{\dagger} \partial_x f_{\sigma}) + f_{\perp} \partial_x f_{\perp}^{\dagger} - f_{\perp}^{\dagger} \partial_x f_{\perp} \right]. \quad (13)$$

Using the coefficients introduced in equations (9), the Josephson current (13) reads

$$I_J = ieN(0)DS\pi T \sum_{\omega,\sigma=\pm} \frac{\lambda_{\sigma}}{2} [A_{\sigma}(\chi)B_{\sigma}(-\chi) - B_{\sigma}(\chi)A_{\sigma}(-\chi)] + \lambda_{\perp} [A_{\perp}(\chi)B_{\perp}(-\chi) - B_{\perp}(\chi)A_{\perp}(-\chi)]. \quad (14)$$

Since the coefficients A_{σ}^j and B_{σ}^j are solutions to the linear system of equations (10) and (11), they are linear combinations of $e^{i\chi}$ and $e^{-i\chi}$. Since the expression (14) is explicitly antisymmetric with respect to $\chi \mapsto -\chi$, it always produces the sinusoidal current-phase relation (1). Finally, the expression (14) does not contain the domain index j : it can be calculated in any of the two domains, and the results must coincide due to the conservation of the supercurrent in the Usadel equations.

In the following sections, this formalism is used to study the influence of a magnetic domain structure on the Josephson current.

III. DOMAINS OF DIFFERENT THICKNESSES IN THE P AND AP CONFIGURATIONS

A. Parallel case (P)

In the most trivial case $\theta = 0$, the equations can be solved easily with $A_{\perp}^j = B_{\perp}^j = 0$. We naturally retrieve the expression reported in Ref. 4 for a single-domain S-F-S trilayer (of thickness $d_1 + d_2$),

$$I_c^P = eN(0)DS\pi T \sum_{\omega,\sigma=\pm} \frac{\Delta^2}{\omega^2} \left[\frac{\lambda_{\sigma}}{\sinh \lambda_{\sigma}(d_1 + d_2)} \right]. \quad (15)$$

The exact summation over the Matsubara frequencies ω can be done numerically. However, in many experimental situations, the exchange field is much larger than T_c . In this limit, we can assume $\hbar \gg \omega$ which implies $\lambda_{\pm} = \frac{1 \mp i}{\xi_F}$. The summation over Matsubara frequencies reduces then to

$$\sum_{\omega} \frac{1}{\omega^2} = \frac{1}{4T^2} \quad (16)$$

and the critical current is given by the simple expression

$$I_c^P = I_0 \text{Re} \left[\frac{1 + i}{\sinh \left[(1 + i) \left(\frac{d_1 + d_2}{\xi_F} \right) \right]} \right] \quad (17)$$

with

$$I_0 = \frac{eN(0)DS\pi\Delta^2}{2\xi_F T}. \quad (18)$$

From Eq. (17) it is clear that the critical current oscillates as a function of the junction length, with a pseudo-period of the order of ξ_F . When the critical current becomes negative, the S-F-S hybrid structure is in the π state.

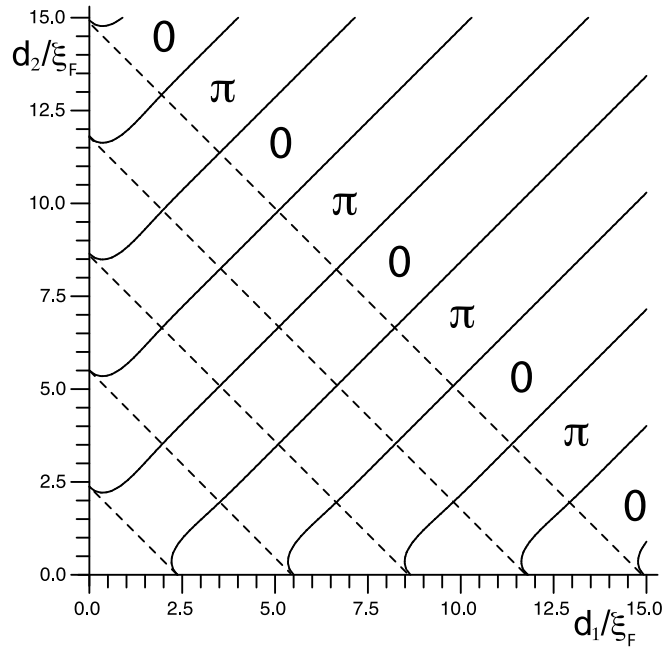


FIG. 2: Quasi-periodic 0 to π transitions for antiparallel (solid lines) and parallel (dashed lines) magnetization. On the graph, the indications 0 and π refer to the antiparallel case. In the parallel case, the transitions occur along lines with $d_1 + d_2 = \text{const}$, starting from the 0 state.

B. Antiparallel case (AP)

In the antiparallel configuration $\theta = \pi$, the exchange field has the opposite direction in the two domains. In this case we again find $A_{\perp}^j = B_{\perp}^j = 0$, and the critical current can be easily derived,

$$I_c^{AP} = I_0 \xi_F T^2 \sum_{\omega, \sigma = \pm} \frac{1}{\omega^2} \left[\frac{2\lambda_{\sigma} \lambda_{-\sigma}}{\lambda_{\sigma} \sinh \lambda_{-\sigma} d_2 \cosh \lambda_{\sigma} d_1 + \lambda_{-\sigma} \cosh \lambda_{-\sigma} d_2 \sinh \lambda_{\sigma} d_1} \right]. \quad (19)$$

In the limit of the large exchange field $h \gg T_c$, the summation over the Matsubara frequencies (16) results in

$$I_c^{AP} = I_0 \text{Re} \left[\frac{2}{\sin(d_+ + id_-) + \sinh(d_+ - id_-)} \right] \quad (20)$$

with

$$d_+ = (d_1 + d_2)/\xi_F \quad (21)$$

$$d_- = (d_1 - d_2)/\xi_F. \quad (22)$$

For plotting the 0- π phase diagram in d_1 - d_2 coordinates we use the condition of the vanishing critical current. From the equations (17) and (20), the critical current vanishes if

$$\sin d_+ \cosh d_+ + \sinh d_+ \cos d_+ = 0 \quad (23)$$

in the parallel case, and if

$$\sin d_+ \cosh d_- + \sinh d_+ \cos d_- = 0 \quad (24)$$

in the antiparallel case. The resulting phase diagram is plotted in Fig. 2.

For $d_1 = d_2 = d$ (symmetric case), we obtain that the critical current is positive for any d : identical F layers in the AP configuration cannot produce the π state (a similar conclusion was drawn in Ref. 18 for ballistic junctions and for diffusive junctions at low temperature). For $d_1 \neq d_2$, the SFF'S junction can be either in the usual 0 state or in the π state depending on the difference between d_1 and d_2 (see Fig. 2). For large d_1 and d_2 , the periodic dependence of the

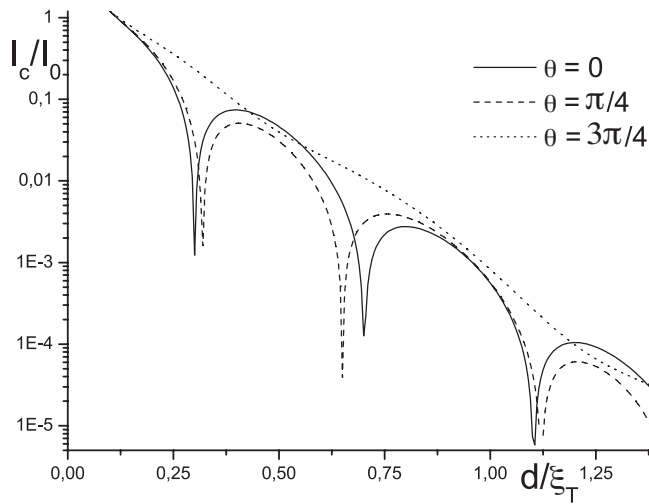


FIG. 3: Critical current dependence on the size of the junction for $\theta = 0, \pi/4$ and $3\pi/4$. We take $h/T = 100$ which corresponds to a realistic value for a diluted ferromagnet, as reported in Ref. 11 and $\xi_T = \sqrt{D/2\pi T}$.

phase transitions on the layer thicknesses approximately corresponds to a single-layer SFS junction of the thickness $|d_1 - d_2| + (\pi/4)\xi_F$. This result is similar to the case of the clean SFF'S junction where the phase compensation arising from the two antiparallel domains is observed.¹⁸

Another interesting feature of the phase diagram in Fig. 2 is the “reentrant” behavior of the phase transition at a very small thickness of one of the layers. If the SFS junction is tuned to a $0-\pi$ transition point, and one adds a thin layer F' of antiparallel magnetization, then a small region of the “opposite” phase (corresponding to increasing the F thickness) appears, before the F-F' compensation mechanism stabilizes the phase corresponding to reducing the F thickness.

In this Section, we have seen that the π state disappears in the antiparallel orientation for geometrically identical F-layers. However, we do not observe an enhancement of the critical current (compared to the zero field current) in the AP configuration such as reported in Refs. 19,23. This is in agreement with the claim of Ref. 19 that this enhancement is present only at low temperatures.

In the next section, we demonstrate that the suppression of the π state occurs continuously as we change the misorientation angle.

IV. ARBITRARY MAGNETIZATION MISORIENTATION AND EQUAL THICKNESSES

In the previous section, we have plotted the phase diagram for arbitrary layer thicknesses d_1 and d_2 in the cases of parallel and antiparallel magnetization. In principle, one can extend this phase diagram to arbitrary misorientation angles θ . Such a calculation amounts to solving a set of linear equations (10) and (11) for the 12 parameters defined in Eq. (9). This calculation is straightforward, but cumbersome, and we consider only the simplest situation with equal layer thicknesses $d_1 = d_2 = d$.

For equal layer thicknesses, the $0-\pi$ transitions are present at $\theta = 0$ and absent at $\theta = \pi$. We will see below that with increasing the misorientation angle θ the amplitude of the critical-current oscillations (as a function of d) decreases, and the π phase progressively shrinks. At a certain “critical” angle θ_c , the π phase disappears completely for any value of d . We find that the critical value is $\theta_c = \frac{\pi}{2}$, surprisingly independent of the strength of the exchange field.

The details of the calculation of the critical current are presented in the Appendix. In the general case, the current can be written in the form of a Matsubara sum such as given in Eq. (A5). In Fig. 3, we plot the current as a function of the domain thickness for different angles performing the summation over Matsubara frequencies numerically using realistic values for the temperature and the exchange field. We find that the domain structure reduces the π -state regions compared to the $\theta = 0$ parallel case as well as the amplitude of the current in this state. To the contrary, the 0 -state regions are extended and the current amplitude is increased in this state. This result may be simply understood as a continuous interpolation between a sign-changing I_c in the single-domain case and an always-positive I_c in the antiparallel case.

Considering the high-exchange-field limit introduced in Sec. III, namely $h \gg T_c$, and assuming further $d \ll \xi_S$

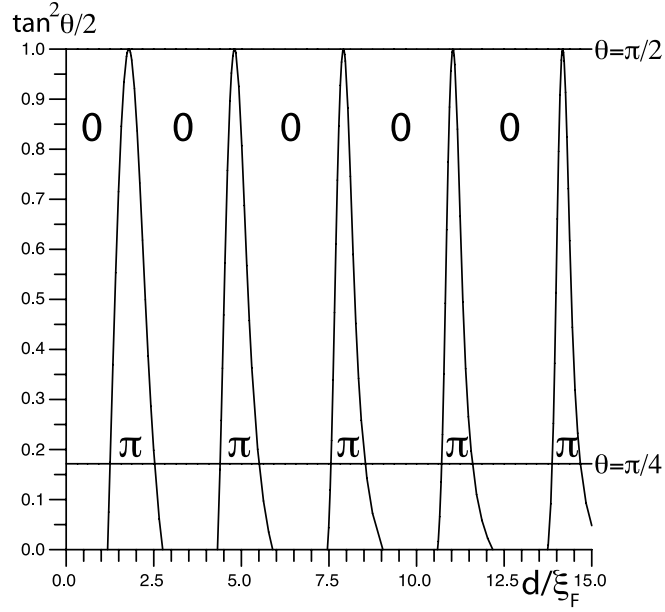


FIG. 4: d - θ phase diagram in the limit of a large exchange field. The dependence on d is almost (but not exactly) periodic.

(which is a reasonable assumption for the first several 0 - π transitions in the high-field limit), we have $\lambda_{\perp} \ll \lambda_{\pm}$ and $\lambda_{\perp}d \ll 1$ so that one can expand Eq. A5) in powers of λ_{\perp} . To the lowest order of expansion, the sum over Matsubara frequencies is done and we obtain

$$I_c(\theta) = 8 \frac{d}{\xi_F} I_0 \frac{(Q_+ + P_+ \tan^2 \frac{\theta}{2})(P_+ + Q_+ \tan^2 \frac{\theta}{2}) - (1 - \tan^4 \frac{\theta}{2})P_- Q_-}{(P_+^2 - P_-^2 + \tan^2 \frac{\theta}{2}(P_+ Q_+ + P_- Q_-))(Q_+^2 - Q_-^2 + \tan^2 \frac{\theta}{2}(P_+ Q_+ + P_- Q_-))}, \quad (25)$$

where P_{\pm} and Q_{\pm} are simple functions of the ratio d/ξ_F ,

$$P_{\pm} = 2 \frac{d}{\xi_F} \left(\cosh(1+i) \frac{d}{\xi_F} \pm \cosh(1-i) \frac{d}{\xi_F} \right)$$

$$Q_{\pm} = (1+i) \sinh(1-i) \frac{d}{\xi_F} \pm (1-i) \sinh(1+i) \frac{d}{\xi_F}. \quad (26)$$

From the general formula (25), one can retrieve the expressions (17) and (20) for the Josephson current in the (symmetric $d_1 = d_2$) parallel and antiparallel cases by setting respectively $\theta = 0$ and $\theta = \pi$. Within the approximation of a high exchange field, the critical current (25) is a ratio of second degree polynomials in the variable $\tan^2 \frac{\theta}{2}$. The critical current cancels if

$$\tan^4 \frac{\theta}{2} (P_+ Q_+ + P_- Q_-) + \tan^2 \frac{\theta}{2} (P_+^2 + Q_+^2) + (P_+ Q_+ - P_- Q_-) = 0. \quad (27)$$

This equation allows one to compute the full S-FF'-S phase diagram in the d - θ coordinates (Fig. 4). We observe that Eq. (27) cannot be satisfied for any thickness as soon as θ exceeds $\frac{\pi}{2}$. As the misorientation angle θ decreases below $\frac{\pi}{2}$, the region of the π state in the phase diagram Fig. 4 increases, and it becomes maximal at $\theta = 0$ (i.e., in the parallel configuration).

Away from the high-exchange-field limit, we can find the value of θ_c numerically using the exact formula, Eq. (A5). Remarkably, our calculations show that the critical value $\theta_c = \frac{\pi}{2}$ remains independent of the strength of the field h .

V. DISCUSSION AND EXPERIMENTAL ASPECTS

The main conclusion of the present work is that a domain structure in the SFS junction reduces the region in the phase space occupied by the π state. We have demonstrated this reduction with the example of the two domains placed along the junction. However we expect that this qualitative conclusion survives for more general configurations

of domains. In view of this reasoning, we suggest that the shift in the $0-\pi$ transition sequence reported in Ref. 11 and attributed to a “dead layer” of the ferromagnet may be alternatively explained by a domain structure in the junction. If such a domain structure slightly reduces the region of the π phase in favor of the 0 phase, this would shift the positions of the two first $0-\pi-0$ transitions in a manner similar to the effect of a “dead layer” (see, e.g., our $\theta = \pi/4$ plot in Fig. 3). To distinguish between the two scenarios, one would need to observe at least three consecutive $0-\pi$ transitions (and/or develop a more realistic theory of the effect of domains in SFS junctions).

Many of our results are based on the high-exchange-field approximation assuming $\xi_S/\xi_F = \sqrt{h/(2\pi T_c)} \gg 1$. This is a reasonable approximation for the type of samples reported in Ref. 11: the exchange field in the CuNi ferromagnetic alloys has been estimated at 850K, whereas the critical temperature of Nb is of the order of 9K. Thus, the ratio ξ_S/ξ_F is of the order of 4. Note that the high-field limit is consistent with the diffusive limit condition $h\tau_e \ll 1$ with τ_e the elastic mean free time (see Ref. 24 for details). The parameters of the experiments¹¹ yield the estimation $h\tau_e \approx 0.1$.

In our treatment we have neglected the finite transparency of the interfaces, the finite mean free path of electrons, the spin-flip and spin-orbit scattering. Of course, those effects may be incorporated in the formalism of Usadel equations in the usual way (see, e.g., Refs. 25,26,27). We expect that they do not change the qualitative conclusion about the reduction of the π state by the domain structure. A realistic quantitative theory of SFS junctions may need to take those effects into account, in addition to a more realistic domain configuration in the ferromagnet.

Acknowledgments

We thank M. Houzet for useful discussions. This work was supported by the Swiss National Foundation.

APPENDIX A: SOLVING THE LINEARIZED USADEL EQUATIONS

To solve the system of linear equations (10) and (11) with the 12 variables $A_{\pm,\perp}^j$ and $B_{\pm,\perp}^j$, it is convenient first to reduce the number of variables by resolving the continuity relations (11) in terms of the 6 variables

$$\begin{aligned}\beta_{\pm} &= B_{\pm}^1 \mp B_{\perp}^1 \tan \frac{\theta}{2} = B_{\pm}^2 \pm B_{\perp}^2 \tan \frac{\theta}{2} \\ \beta_{\perp} &= B_{\perp}^1 + \frac{B_{+}^1 - B_{-}^1}{2} \tan \frac{\theta}{2} = B_{\perp}^2 - \frac{B_{+}^2 - B_{-}^2}{2} \tan \frac{\theta}{2} \\ \alpha_{\pm} &= \lambda_{\pm} A_{\pm}^1 \mp \lambda_{\perp} A_{\perp}^1 \tan \frac{\theta}{2} = \lambda_{\pm} A_{\pm}^2 \pm \lambda_{\perp} A_{\perp}^2 \tan \frac{\theta}{2} \\ \alpha_{\perp} &= \lambda_{\perp} A_{\perp}^1 + \frac{\lambda_{+} A_{+}^1 - \lambda_{-} A_{-}^1}{2} \tan \frac{\theta}{2} = \lambda_{\perp} A_{\perp}^2 - \frac{\lambda_{+} A_{+}^2 - \lambda_{-} A_{-}^2}{2} \tan \frac{\theta}{2}.\end{aligned}\tag{A1}$$

Solving now the set of 6 equations (10) produces the solution

$$\begin{aligned}\alpha_{\perp} &= \frac{2\Delta}{\omega} \lambda_{+} \lambda_{-} \lambda_{\perp} \cosh(\lambda_{\perp} d) \frac{p_{-}}{p_{+}^2 - p_{-}^2 + \tan^2 \frac{\theta}{2} (p_{+} q_{+} + p_{-} q_{-})} \tan \frac{\theta}{2} (1 + \tan^2 \frac{\theta}{2}) \cos \chi \\ \beta_{+} - \beta_{-} &= -\frac{4\Delta}{\omega} \lambda_{+} \lambda_{-} \sinh(\lambda_{\perp} d) \frac{p_{-}}{p_{+}^2 - p_{-}^2 + \tan^2 \frac{\theta}{2} (p_{+} q_{+} + p_{-} q_{-})} (1 + \tan^2 \frac{\theta}{2}) \cos \chi \\ \beta_{+} + \beta_{-} &= \frac{4\Delta}{\omega} \lambda_{+} \lambda_{-} \sinh(\lambda_{\perp} d) \frac{p_{+} + \tan^2 \frac{\theta}{2} q_{+}}{p_{+}^2 - p_{-}^2 + \tan^2 \frac{\theta}{2} (p_{+} q_{+} + p_{-} q_{-})} \cos \chi \\ \alpha_{+} - \alpha_{-} &= -\frac{4i\Delta}{\omega} \lambda_{+} \lambda_{-} \lambda_{\perp} \cosh(\lambda_{\perp} d) \frac{q_{-}}{q_{+}^2 - q_{-}^2 + \tan^2 \frac{\theta}{2} (p_{+} q_{+} + p_{-} q_{-})} (1 + \tan^2 \frac{\theta}{2}) \sin \chi \\ \alpha_{+} + \alpha_{-} &= -\frac{4i\Delta}{\omega} \lambda_{+} \lambda_{-} \lambda_{\perp} \cosh(\lambda_{\perp} d) \frac{q_{+} + \tan^2 \frac{\theta}{2} p_{+}}{q_{+}^2 - q_{-}^2 + \tan^2 \frac{\theta}{2} (p_{+} q_{+} + p_{-} q_{-})} \sin \chi \\ \beta_{\perp} &= \frac{2i\Delta}{\omega} \lambda_{+} \lambda_{-} \sinh(\lambda_{\perp} d) \frac{q_{-}}{q_{+}^2 - q_{-}^2 + \tan^2 \frac{\theta}{2} (p_{+} q_{+} + p_{-} q_{-})} \tan \frac{\theta}{2} (1 + \tan^2 \frac{\theta}{2}) \sin \chi,\end{aligned}\tag{A2}$$

where

$$\begin{aligned}p_{\pm} &= \lambda_{+} \lambda_{-} \sinh \lambda_{\perp} d (\cosh \lambda_{+} d \pm \cosh \lambda_{-} d) \\ q_{\pm} &= \lambda_{\perp} \cosh \lambda_{\perp} d (\lambda_{+} \sinh \lambda_{-} d \pm \lambda_{-} \sinh \lambda_{+} d).\end{aligned}\tag{A3}$$

In terms of the new variables, the supercurrent (14) becomes

$$I_J = ieN(0)DS\pi T \sum_{\omega} \left[\frac{1}{4}(\alpha_+ + \alpha_-)(\chi)(\beta_+ + \beta_-)(-\chi) + \frac{1}{4(1 + \tan^2 \frac{\theta}{2})}(\alpha_+ - \alpha_-)(\chi)(\beta_+ - \beta_-)(-\chi) + \frac{\alpha_{\perp}(\chi)\beta_{\perp}(-\chi)}{1 + \tan^2 \frac{\theta}{2}} \right] - [\chi \leftrightarrow -\chi]. \quad (\text{A4})$$

The resulting current-phase relation is sinusoidal with the critical current

$$I_c(\theta) = 4I_0\xi_F T^2 \sum_{\omega} \frac{(\lambda_+ \lambda_-)^2 \lambda_{\perp} \sinh 2\lambda_{\perp} d}{\omega^2} \times \frac{(q_+ + p_+ \tan^2 \frac{\theta}{2})(p_+ + q_+ \tan^2 \frac{\theta}{2}) - (1 - \tan^4 \frac{\theta}{2})p_- q_-}{(p_+^2 - p_-^2 + \tan^2 \frac{\theta}{2}(p_+ q_+ + p_- q_-))(q_+^2 - q_-^2 + \tan^2 \frac{\theta}{2}(p_+ q_+ + p_- q_-))}. \quad (\text{A5})$$

Eq. (A5) can be used for numerical calculations of the critical current for an arbitrary relative orientation of the ferromagnetic exchange fields and for any value of their magnitude (e.g., for producing the plot in Fig. 3). In the body of the article, a simpler expression for the current is given in the high-exchange-field limit (Eq. (25)).

- ¹ I. Zutic, J. Fabian, and S. D. Sarma, *Rev. Mod. Phys.* **76**, 323 (2004).
- ² L. B. Ioffe, V. B. Geshkenbein, M. V. Feigelman, A. L. Fauchere, and G. Blatter, *Nature* **398**, 679 (1999).
- ³ L. B. Ioffe, M. V. Feigel'man, A. Ioselevich, D. Ivanov, M. Troyer, and G. Blatter, *Nature* **415**, 503 (2002).
- ⁴ A. I. Buzdin, *Rev. Mod. Phys.* **77**, 935 (2005).
- ⁵ E. A. Demler, G. B. Arnold, and M. R. Beasley, *Phys. Rev. B* **55**, 15174 (1997).
- ⁶ L. N. Bulaevskii, V. V. Kuzii, and A. A. Sobyenin, *Pis'ma Zh. Eksp. Teor. Fiz.* **25**, 314 (1977), [*JETP Lett.* **25**, 290 (1977)].
- ⁷ T. Yamashita, K. Tanikawa, S. Takahashi, and S. Maekawa, *Phys. Rev. Lett.* **95**, 097001 (2005).
- ⁸ T. Kontos, M. Aprili, J. Lesueur, F. Genet, B. Stephanidis, and R. Boursier, *Phys. Rev. Lett.* **89**, 137007 (2002).
- ⁹ V. V. Ryazanov, V. A. Oboznov, A. Y. Rusanov, A. V. Veretennikov, A. A. Golubov, and J. Aarts, *Phys. Rev. Lett.* **86**, 2427 (2001).
- ¹⁰ V. V. Ryazanov, V. A. Oboznov, A. S. Prokofiev, V. V. Bolginov, and A. K. Feofanov, *J. Low Temp. Phys.* **136**, 385 (2004).
- ¹¹ V. A. Oboznov, V. V. Bol'ginov, A. K. Feofanov, V. V. Ryazanov, and A. I. Buzdin, *Phys. Rev. Lett.* **96**, 197003 (2006).
- ¹² G. Eilenberger, *Z. Phys.* **214**, 195 (1968).
- ¹³ K. D. Usadel, *Phys. Rev. Lett.* **25**, 507 (1970).
- ¹⁴ A. A. Golubov, M. Y. Kupriyanov, and E. Il'ichev, *Rev. Mod. Phys.* **76**, 411 (2004).
- ¹⁵ A. I. Buzdin, L. N. Bulaevskii, and S. V. Panyukov, *Pis'ma Zh. Eksp. Teor. Fiz.* **35**, 147 (1982), [*JETP Lett.* **35**, 178 (1982)].
- ¹⁶ A. I. Buzdin and M. Y. Kupriyanov, *Pis'ma Zh. Eksp. Teor. Fiz.* **53**, 308 (1991), [*JETP Lett.* **53**, 321 (1991)].
- ¹⁷ F. S. Bergeret, A. F. Volkov, and K. B. Efetov, *Phys. Rev. B* **64**, 134506 (2001).
- ¹⁸ Y. M. Blanter and F. W. J. Hekking, *Phys. Rev. B* **69**, 024525 (2004).
- ¹⁹ V. N. Krivoruchko and E. A. Koshina, *Phys. Rev. B* **64**, 172511 (2001).
- ²⁰ F. S. Bergeret, A. F. Volkov, and K. B. Efetov, *Rev. Mod. Phys.* **77**, 1321 (2005).
- ²¹ D. A. Ivanov and Y. V. Fominov, *Phys. Rev. B* **73**, 214524 (2006).
- ²² M. Y. Kupriyanov and V. F. Lukichev, *Zh. Eksp. Teor. Fiz.* **94**, 139 (1988), [*Sov. Phys. JETP* **67**, 1163 (1988)].
- ²³ F. S. Bergeret, A. F. Volkov, and K. B. Efetov, *Phys. Rev. Lett.* **86**, 3140 (2001).
- ²⁴ N. Kopnin, *Theory of nonequilibrium superconductivity* (Oxford University Press, 2001).
- ²⁵ E. A. Koshina and V. N. Krivoruchko, *Zh. Eksp. Teor. Fiz.* **71**, 182 (2000), [*JETP Lett.* **71**, 123 (2000)].
- ²⁶ A. Buzdin and I. Baladie, *Phys. Rev. B* **67**, 184519 (2003).
- ²⁷ M. Fauré, A. I. Buzdin, A. A. Golubov, and M. Y. Kupriyanov, *Phys. Rev. B* **73**, 064505 (2006).